Journal of Solid State Chemistry **168,** 653–660 (2002)
doi:10.1006/jssc.2002.9763

A New Conducting Molecular Solid Based on the Magnetic $[Ni(dmf)_6]^{2+}$ Cation and on $[Ni(dsit)_2]_2^{2-}$ (dsit=1,3-dithiole-2-thione-4,5-diselenolate) Showing an Unprecedented Anion Packing

S. Curreli,* P. Deplano,* M.L. Mercuri,*,[1] L. Pilia,* A. Serpe,* F. Bigoli,† M.A. Pellinghelli,† E. Coronado,‡ C.J. Gómez-García,‡,[1] and E. Canadell§

*Dipartimento di Chimica Inorganica e Analitica, Università di Cagliari, S.S. 554, Bivio per Sestu, I09042 Monserrato, Cagliari, Italy; †Dipartimento di Chimica Generale ed Inorganica, Chimica Analitica, Chimica Fisica, Università di Parma, Parco Area delle Scienze 17A, I-43100 Parma, Italy; ‡Instituto de Ciencia Molecular (ICMol), Universidad de Valencia, C/Dr. Moliner 50, E-46100 Burjasot, Valencia, Spain; and §ICMAB (CSIC), Campus de la UAB, 08193 Bellaterra, Spain

Received January 28, 2002; in revised form March 24, 2002; accepted March 27, 2002

The synthesis, X-ray structure, magnetic and transport properties of the compound $Ni(dmf)_6[Ni(dsit)_2]_2$ (dmf = dimethylformamide, dsit = 1,3-dithiole-2-thione-4,5-diselenolate) are described. This compound crystallizes in the monoclinic space group $P2_1/c$, with $a = 18.709(6)$, $b = 22.975(5)$, $c = 20.418(5)$ Å, $\beta = 99.31(2)^\circ$ and $Z = 6$; its structure consists of $[Ni(dsit)_2]_2^{2-}$ dimers and isolated $[Ni(dmf)_6]^{2+}$ cations both centrosymmetric and non-centrosymmetric. The dimers are packed forming chains along the [101] direction with short Se···Se interdimer contacts. Additional interchains S···S contacts render this structure a three-dimensional character, never observed so far in other $[Ni(dsit)_2]^-$ salts. This compound exhibits semiconducting behavior with a room temperature conductivity ($1\,S\,cm^{-1}$) much higher than those reported for other salts of the $[Ni(dsit)_2]^-$ anion. Tight-binding band structure calculations were used to analyze the origin of the semiconducting properties of this salt. The magnetic susceptibility shows Curie behavior with $C = 1.25$ emu K mol^{-1}, typical of isolated Ni(II) ions as expected for the octahedrally coordinated $[Ni(dmf)_6]^{2+}$ cations. © 2002 Elsevier Science (USA)

Key Words: **molecular conductors; dsit; magnetic properties; band structure calculations; $M(dsit)_2$ complexes; diselenolenes.**

INTRODUCTION

Since the discovery of the first molecular superconductor containing a bis(dithiolene) transition metal complex, (TTF)[Ni(dmit)$_2$] (TTF = tetrathiafulvalene, dmit = 1,3-dithiole-2-thione-4,5-dithiolate) (1), a large amount of work has gone into the synthesis and characterization of bis(dithiolene) metal complexes based on the dmit ligand. These fully planar and extensively electron-delocalized M(dmit)$_2$ systems are able to stack in a 1-D "pocker-chip" like way with large intermolecular orbital overlaps between the sulfur atoms thus being suitable for the synthesis of highly conducting materials. In fact, a large amount of conducting compounds and even superconductors have been synthesized and fully characterized by modifying the counterions and/or the metal ions (2). Moreover, dmit offers further possibilities for chemical modifications such as the substitution of the sulfur atoms with selenium atoms in the periphery of the ligand itself or in the dithiolene core of the M(dmit)$_2$ complexes. These substitutions are expected to result in increased polarizabilities and orbital overlaps between molecules, leading to an enhancement in the dimensionality of the solid. Over the past few years, various selenium analogs of dmit have been prepared and among them the dsit ligand (dsit = 1,3-dithiole-2-thione-4,5-diselenolate) has been the most studied (3–14). As far as we know, five M(dsit)$_2$ (M = Ni, Pd) systems have been fully characterized through X-ray studies and electrical properties (Table 1). They all consist of tightly bound dimers with closed-shell tetrahedral cations (5–7). Only in the $[NMe_4][M(dsit)_2]_2$ (M = Ni, Pd) salts, that contain the mixed-valence dimer $[M(dsit)_2]_2^-$, high room temperature conductivities have been observed (~ 36 and $\sim 50\,S\,cm^{-1}$, respectively), although they behave as semiconductors. The other reported salts contain the fully charged $[Ni(dsit)_2]_2^{2-}$ anion and are insulators.

We report in this paper the synthesis, crystal structure and physical properties of the first example of a salt formed

[1] To whom all correspondence should be address. E-mail: mercuri@unica.it, carlos.gomez@uv.es.

0022-4596/02 $35.00

TABLE 1
Complexes of General Formula $(Z)_n[M(dsit)_2]_2$

M	*Z*	*n*	$\sigma_{300\,K}$ ($S\,cm^{-1}$)	Ref.
Ni	Me_4N[a]	0.5	1.3 powder; 36, crystal	(1–4)
	Me_4P	0.5	19, crystal	(3, 4)
	Me_4N	1	4×10^{-3}, powder	(1, 2)
	Et_4N[a]	1	5×10^{-5}, crystal	(3, 4)
	Bu_4N (α-phase)[a]	1	Low	(5, 14)
	Bu_4N (β-phase)[a]	1	Low	(5, 14)
Pd	Me_4N[a]	0.5	30-70, crystal	(1, 2, 8, 9)
	Me_4N	1	4×10^{-2}, powder	(2)
	Me_4N	1.5	4.6×10^{-4}, powder	(2)
Pt	Me_4N	0.5	5.4×10^{-2}, powder	(1, 2)
	Me_4N	1.5	5×10^{-5}, powder	(2)

[a]Compounds whose crystal structures have been reported.

by the $[Ni(dsit)_2]_2^{2-}$ dianion and the transition metal complex $[Ni(dmf)_6]^{2+}$ (dmf = dimethylformamide).

EXPERIMENTAL

Synthesis

The precursor salt $(NBu_4)_2[Ni(dsit)_2]$ was prepared as previously described (13) and recrystallized from acetone/isopropanol prior to use. 0.1 g (0.097 mmol) of $(NBu_4)_2[Ni(dsit)_2]$ was dissolved in dmf (30 mL) yielding a blue–green solution. I_2 (13 mg, 0.051 mmol) in dmf (20 mL) was added dropwise and the resulting olive-green mixture was stirred for 10 min and, after filtration to remove a brown powder, was stored at −18°C. After 24 h, shiny black crystals suitable for X-ray studies were obtained (40% yield). Elem. Anal.: % calculated (found) for $C_{30}H_{42}N_6O_6S_{12}Se_8Ni_3$: C = 20.30 (20.75); H = 2.38 (2.11); N = 4.73 (4.94); S = 21.67 (21.13). IR spectrum (cm^{-1}, KBr pellet): ~4600 br, 1644vs, 1493w, 1432w, 1404w, 1375 m, 1252w, 1110mw, 1063vs, 1022mw, 853vw, 720w, 689w, 512mw, 444vw, 427mw, 375mw.

SINGLE CRYSTAL X-RAY DIFFRACTION

Crystal data

$C_{30}H_{42}N_6Ni_3O_6S_{12}Se_8$, $M = 5325.68$, monoclinic, space group $P2_1/c$ (no. 14), $a = 18.709(6)$, $b = 22.975(5)$, $c = 20.418(5)$ Å, $\beta = 99.31(2)^\circ$ $V = 8661(4)$ Å^3, $T = 293(1)$ K, $Z = 6$, 13,247 reflections measured, 12,850 unique ($R_{int} = 0.0749$), which were used in all calculations. Shiny black needles. Crystal dimensions = $0.12 \times 0.18 \times 0.31$ mm^3. $\mu(CuK\alpha) = 11.327\,mm^{-1}$. The final $R[I > 2\sigma(I)]$ was 0.0705, $wR(F^2) = 0.2114$. Crystallographic data were recorded on a Siemens AED diffractometer using graphite monochromated Cu$K\alpha$ radiation ($\lambda = 1.541838$ Å). An absorption correction was applied after the last isotropic refinement cycle following the empirical method of Walker and Stuart (14) (transmission coefficients 0.503–1.000). The structure was solved by direct methods through Sir92 (15) program and refined by full-matrix least-squares against F^2 using SHELXL-97 (16) program with anisotropic thermal parameters for the non-hydrogen atoms of both anions and the metal atoms of the cations only. The hydrogen atoms were placed in idealized calculated positions and allowed to ride on their carbon atom. The bonds lengths and angles are given in Table 3.

Band Structure Calculations

Both the tight-binding band structure and molecular calculations used an extended Hückel hamiltonian (17) and a modified Wolfsberg–Helmholtz formula (18) to calculate the non-diagonal H_{ij} matrix elements. Double-ζ type orbitals for Ni 3*d* and single-ζ type for C 2*s* and 2*p*, S 3*s* and 3*p*, Se 4*s* and 4*p*, H 1*s* and Ni 4*s* and 4*p* were used. The exponents and parameters used in the calculations were taken from previous work (19, 20).

Spectroscopic Measurements

IR spectra (300–8000 cm^{-1}) were recorded on a Bruker IFS55 spectrometer working at room pressure and using a flow of dried air. Electronic spectra (300–2000 nm) were recorded on KBr pellets with a Cary 5 spectrophotometer, equipped with a diffuse reflectance accessory.

Conductivity Measurements

D.C. conductivity measurements over the range 25–300 K were performed with the standard four contacts method on the best developed face of two different single crystals with applied D.C. currents of 10, 100 and 1000 nA, giving reproducible and very similar results for both crystals. Contacts to the crystals were made by platinum wires (25 μm diameter) attached by graphite paste to the samples.

Magnetic Measurements

Variable temperature susceptibility measurements were carried out in the temperature range 2–300 K at a magnetic field of 1 T on polycrystalline samples with a magnetometer (Quantum Design MPMS-XL-5) equipped with a SQUID sensor. The susceptibility data were corrected for the sample holders previously measured in the same conditions and for the diamagnetic contributions of the salts as deduced by using Pascal's constant tables. Room tempera-

ture ESR spectra were recorded on a polycrystalline sample at X–band with a Bruker E500 ELEXSYS spectrometer.

RESULTS AND DISCUSSION

Synthesis and Crystal Structure

By reacting $(NBu_4)_2[Ni(dsit)_2]$ with I_2 in dmf, a compound that can be formulated as $[Ni(dmf)_6][Ni(dsit)_2]_2$ on the basis of analytical results is obtained (Scheme 1). The reaction solvent has been selected in order to favor the oxidation process to the monoanion, since previous electrochemical studies performed in different solvents (2) have shown that the oxidation is easier in dmf ($E = -0.070$ V vs SCE).

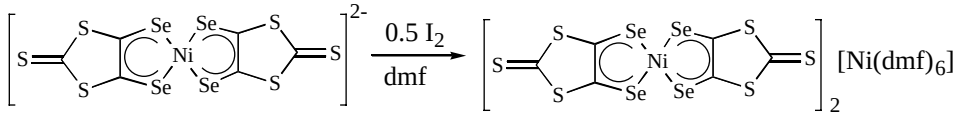

SCHEME 1.

The obtained compound shows an unprecedented structure that consists of $[Ni(dsit)_2]_2^{2-}$ dimers and isolated $[Ni(dmf)_6]^{2+}$ cations. In the unit-cell, there are two different $[Ni(dsit)_2]_2^{2-}$ dimers: a centrosymmetric one (AA) formed by two $[Ni(dsit)_2]^-$ units of the same type (A), and a non-centrosymmetric dimer (BC) which contains two crystallographically different $[Ni(dsit)_2]^-$ units (B and C) (Fig. 1). There is also a centrosymmetric and a non-centrosymmetric $[Ni(dmf)_6]^{2+}$ cation (Fig. 1).

The $[Ni(dsit)_2]_2^{2-}$ dimers show the typical structural arrangement adopted by this unit in previously reported salts (4, 5) Each nickel is coordinated by five selenium atoms, two from each of the two chelating ligands (in an almost square planar arrangement), and one from the other $[Ni(dsit)_2]^-$ unit in the axial position (Fig. 1). This coordination mode leads to a distorted square pyramidal site for Ni(II) and to a nickel-over-selenium overlap between the $[Ni(dsit)_2]^-$ units. Both the axial and the equatorial Ni–Se bond distances are in the range of those found in the three structurally characterized $[Ni(dsit)_2]_2^{2-}$ dimers (Table 2) (4, 5).

The $[Ni(dsit)_2]^-$ units appear slightly distorted from the planar geometry. Thus, in unit A, one dsit is nearly planar while the other is slightly puckered and twisted out of the plane of the former (Fig. 1). The nickel atom lies almost in the plane of the planar dsit (0.030 Å from it) and it is at 0.355 Å from the average plane of the other dsit. This arrangement is very similar in units B and C. The only difference is that in B and C the two dsits are nearly planar, leading to BC dimers with almost parallel $[Ni(dsit)_2]^-$ anions (the dihedral angle between the average planes is only 2.0°). The distances from the nickel atoms to the average planes of the two dsits are 0.108 and 0.657 Å in the B unit and 0.184 and 0.579 Å in the C unit. A slightly lengthening of the Se–C bond distances [range 1.825(14)–1.901(14) Å] involved in the dimerization is observed while the exocyclic C–S and the C–C bond lengths fall in the expected range (Table 3). These distances are also similar to those found in the three structurally characterized $[Ni(dsit)_2]_2^{2-}$ dimers (4, 5).

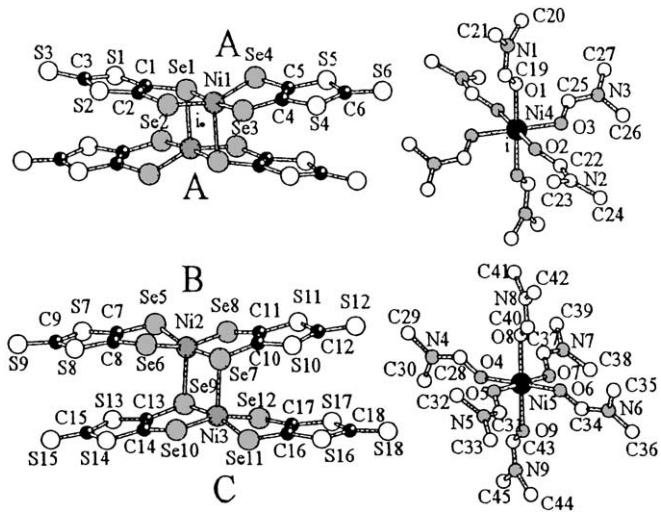

FIG. 1. Molecular structure of the centrosymmetric (AA) and non-centrosymmetric (BC) $[Ni(dsit)_2]_2^{2-}$ dimers and of the two different $[Ni(dmf)_6]^{2+}$ cations showing the labelling scheme.

The dimers present several intradimer Se···Se contacts (3.44 and 3.61 Å in AA and BC dimers, respectively), much shorter than the sum of the Van der Waals radii of the selenium atoms (3.80 Å). The distance between the average planes of the $Ni(dsit)_2$ units in the AA dimer is longer than in the BC dimer (3.545 Å compared to 3.368 Å, respectively). These intradimer distances are also similar to those found in the other $[Ni(dsit)_2]^-$ salts (see Table 2).

An interesting structural feature of the title salt is the presence of several short interdimer Se···Se contacts: 3.59 Å between the AA and BC dimers and 3.67 Å between

TABLE 2
Ni–Se Bond Distances, Interplanar Distances and Shortest Intradimer Se···Se Contacts (Å) in the Salts $(Z)_n[Ni(dsit)_2]_2$ ($n = 2$, $Z = NEt_4^+$, [4] NBu_4^+; [5] $n = 1$, $Z = Ni(dmf)_6^{2+}$)

		$Z = NBu_4^+$		$Z = Ni(dmf)_6^{2+}$		
Atoms	$Z = NEt_4^+$	α-phase	β-phase	A unit	B unit	C unit
Ni–Se_{equat}	2.338(2)	2.347(1)	2.334(2)	2.319(3)	2.335(3)	2.317(3)
Ni–Se_{equat}	2.337(2)	2.336(1)	2.344(2)	2.338(3)	2.355(3)	2.319(3)
Ni–Se_{equat}	2.345(2)	2.317(1)	2.335(2)	2.352(3)	2.316(3)	2.331(3)
Ni–Se_{equat}	2.350(2)	2.316(1)	2.317(2)	2.337(3)	2.320(3)	2.360(3)
Ni–Se_{axial}	2.495(2)	2.480(1)	2.472(2)	2.492(3)	2.509(3)	2.533(3)
Intradimer distances						
Plane–Plane	3.42	3.34	3.29	3.54		3.37
Se···Se	3.548	3.452	3.493	3.440		3.610

the BC ones. These contacts lead to a strong one-dimensional (1-D) character in the anionic sublattice with the dimers packed along the [101] direction having dihedral angles of ca 30° (Fig. 2). This is an unprecedented feature that contrasts with the lack of interdimer contacts found in the other three structurally characterized $[Ni(dsit)_2]^-$ salts (4, 5). As we will see later on, it has significant consequences in the transport properties of the material. The chain of $[Ni(dsit)_2]_2^{2-}$ dimers follows the sequence:···(AA)(BC)(CB) ···. These chains are surrounded by four parallel chains of $[Ni(dmf)_6]^{2+}$ cations and four chains of $[Ni(dsit)_2]_2^{2-}$ dimers in a chessboard-like arrangement in such a way that this structure can be viewed as formed by chains of $[Ni(dsit)_2]_2^{2-}$ anions inserted inside the tunnels formed by four chains of $[Ni(dmf)_6]^{2+}$ cations and vice versa (Figs. 3 and 4).

Another remarkable feature of this structure is the presence of short S···S interchain contacts: each anionic chain is connected to the four neighbors anionic chains with two S···S contacts (3.49 and 3.59 Å) shorter than sum of the Wan der Waals radii (3.60 Å). These extra contacts render this structure an unprecedented three-dimensional 3-D character that strongly contrasts with the zero dimensionality (isolated dimers) found in the three other structurally characterized $[Ni(dsit)_2]^-$ salts (4, 5).

Both, the centrosymmetric and the non-centrosymmetric $[Ni(dmf)_6]^{2+}$ cations, (Fig. 1) show a quite regular octahedral coordination around the metal atom, each dmf molecule acting as a monodentate ligand via the O atom. Thus, the Ni–O bond distances range from 2.047 to 2.059 Å in the centrosymmetric cation and from 2.016 to 2.062 Å in the non-centrosymmetric one. The O–Ni–O bond angles are also very close to 90°. The bond lengths in these complexes are similar to those reported for the analogous perchlorate (21) and tetrafluroborate (22) salts. As observed in the last compounds, where two independent metal sites are present too, the equatorial dmf molecules form weak hydrogen-bonds involving each O atom and the amide C–H of a neighboring ligand (C···O = 2.99(2)–3.04(2) Å, O···H = 2.472–0.54 Å, C–H···O = 115–117°). Finally, it is interesting to note that there are several short anion-cation contacts with a shortest C···S distance of 3.399 Å (C44···S5).

The IR spectrum shows the expected bands for this salt. Besides the strong band related to the dmf of the cations (1644 cm^{-1}), the most significant band is found at 1375 cm^{-1}. This band is assigned to the ν(C=C) stretching

TABLE 3
Selected Bond Lengths (Å) and Angles (deg) in the $[Ni(dsit)_2]_2^{2-}$ Anions in the $[Ni(dmf)_6][Ni(dsit)_2]_2$ Salt

Non-centrosymmetric		*Centrosymmetric*	
Ni(2)–Se(5)	2.335(3)	Ni(1)–Se(1)	2.319(3)
Ni(2)–Se(6)	2.355(3)	Ni(1)–Se(2)	2.338(3)
Ni(2)–Se(7)	2.316(3)	Ni(1)–Se(3)	2.352(3)
Ni(2)–Se(8)	2.320(3)	Ni(1)–Se(4)	2.337(3)
Ni(2)–Se(9)	2.509(3)	Ni(1)–Se(1')	2.492(3)
Ni(3)–Se(9)	2.317(3)		
Ni(3)–Se(10)	2.319(3)		
Ni(3)–Se(11)	2.331(3)		
Ni(3)–Se(12)	2.360(3)		
Ni(3)–Se(7)	2.533(3)		
Se(5)–Ni(2)–Se(6)	91.66(9)	Se(1)–Ni(1)–Se(2)	92.42(9)
Se(5)–Ni(2)–Se(7)	167.39(12)	Se(1)–Ni(1)–Se(3)	174.30(12)
Se(5)–Ni(2)–Se(8)	84.12(9)	Se(1)–Ni(1)–Se(4)	84.17(9)
Se(5)–Ni(2)–Se(9)	96.30(10)	Se(1)–Ni(1)–Se(1')	94.91(9)
Se(6)–Ni(2)–Se(7)	86.65(9)	Se(2)–Ni(1)–Se(3)	88.90(9)
Se(6)–Ni(2)–Se(8)	161.23(12)	Se(2)–Ni(1)–Se(4)	154.91(12)
Se(6)–Ni(2)–Se(9)	103.31(10)	Se(2)–Ni(1)–Se(1')	96.49(9)
Se(7)–Ni(2)–Se(8)	93.49(9)	Se(3)–Ni(1)–Se(4)	92.30(9)
Se(7)–Ni(2)–Se(9)	96.24(9)	Se(3)–Ni(1)–Se(1')	90.45(9)
Se(8)–Ni(2)–Se(9)	95.33(9)	Se(4)–Ni(1)–Se(1')	108.55(10)
Se(9)–Ni(3)–Se(10)	92.92(10)		
Se(9)–Ni(3)–Se(11)	166.71(12)		
Se(9)–Ni(3)–Se(12)	87.66(9)		
Se(9)–Ni(3)–Se(7)	95.55(9)		
Se(10)–Ni(3)–Se(11)	83.87(9)		
Se(10)–Ni(3)–Se(12)	162.73(12)		
Se(10)–Ni(3)–Se(7)	94.83(9)		
Se(11)–Ni(3)–Se(12)	91.63(10)		
Se(11)–Ni(3)–Se(7)	97.56(10)		
Se(12)–Ni(3)–Se(7)	102.30(10)		
	Range	Range	
C–Se	1.825(14)–1.870(15)	1.861(14)–1.867(14)	
C–$Se_{bridg.}$	1.894(16)–1.901(14)	1.901(14)	
C–Se_{endo}	1.719(16)–1.792(13)	1.708(13)–1.758(17)	
C–Se_{exo}	1.604(16)–1.636(16)	1.594(15)–1.632(16)	
C–C	1.301(17)–1.353(19)	1.331(18)–1.348(18)	
Ni–Se–Ni	83.85(9)–84.36(9)	85.09(9)	
Ni–Se–C	97.1(4)–104.3(4)	96.8(4)–101.4(4)	

Note. Symmetry transformation used to generate equivalent atoms: ('): $-x+1, -y+1, -z+1$.

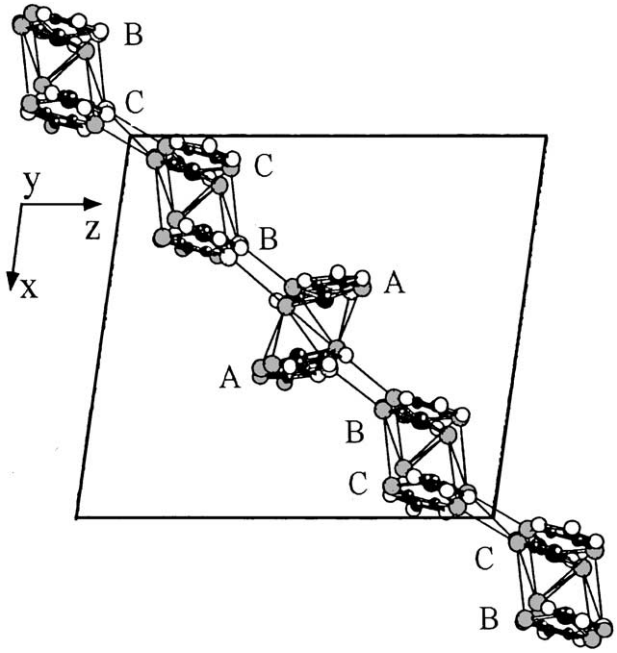

FIG. 2. One-dimensional packing along the [101] direction of the $[Ni(dsit)_2]_2^{2-}$ dimers following the sequence $\cdots(AA)(BC)(CB)\cdots$. Thin lines indicate the intra- and inter-dimer Se···Se contacts shorter than 4.0 Å.

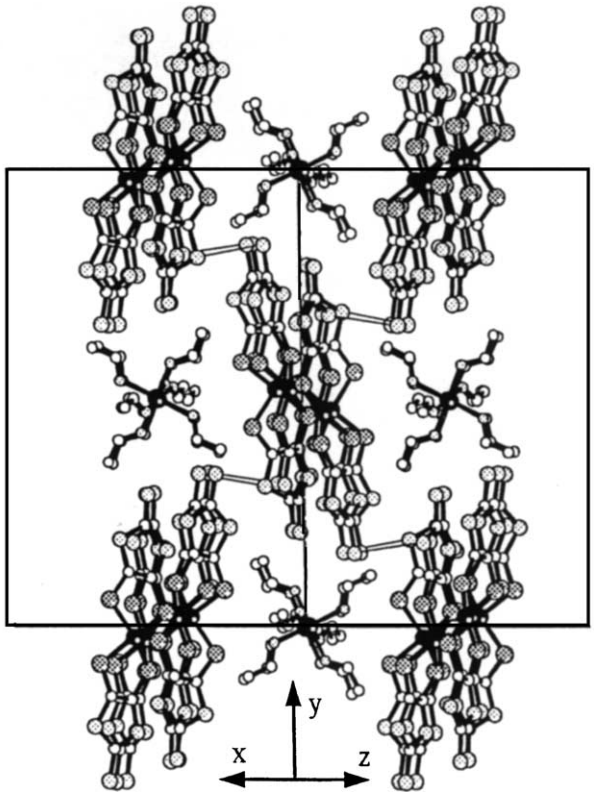

FIG. 3. View of the chain of $[Ni(dsit)_2]_2^{2-}$ dimers surrounded by the four $[Ni(dmf)_6]^{2+}$ chains and four chains of $[Ni(dsit)_2]_2^{2-}$ dimers in a chessboard arrangement.

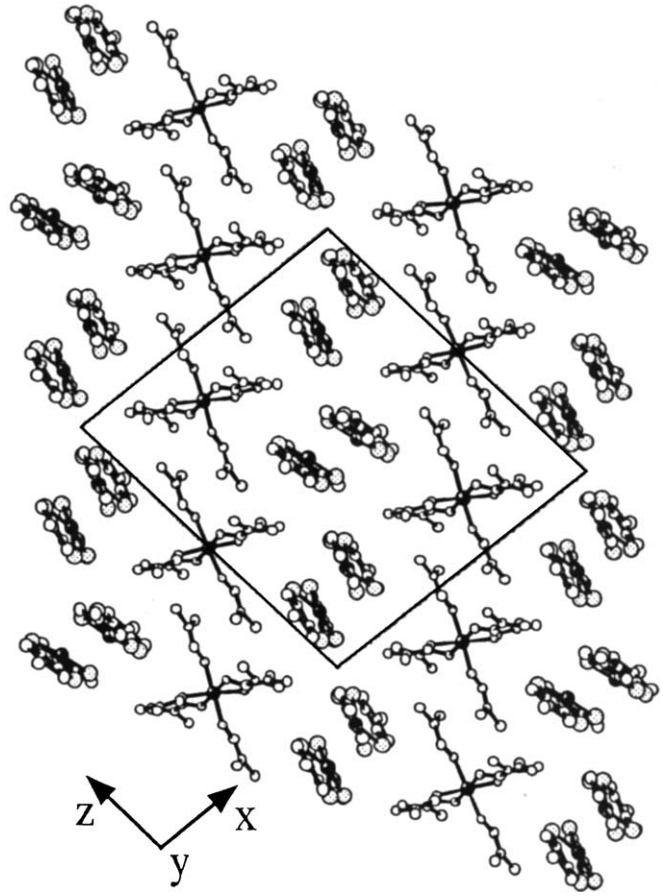

FIG. 4. View of the *ac* plane showing the parallel chains of anions and cations running in the [101] direction.

vibration, which is known to exhibit a linear dependence on the charge in the $Ni(dmit)_2$ system (23). According to this correlation and previous data on $(NBu_4)[Ni(dsit)_2]$ (12), its position is in agreement with the assignment of a -1 charge *per* $Ni(dsit)_2$ unit. The IR spectrum also shows, in the NIR region, a very broad band centered at $\sim 4600\,cm^{-1}$, which can be related to the conducting properties of this salt. This band is also observed in the diffuse reflectance spectrum as a shoulder of the π—π^* band of the $Ni(dsit)_2$ unit, which appears at $\sim 10{,}000\,cm^{-1}$, both in dmf solution and in solid state.

Electrical Properties

The D.C. conductivity of the $[Ni(dmf)_6][Ni(dsit)_2]_2$ salt shows a room temperature conductivity of 1.0–1.2 $S\,cm^{-1}$ and a semiconducting behavior with a small activation energy of 35 meV (Fig. 5). The room temperature conductivity is much higher than that reported for other salts of the $[Ni(dsit)_2]^-$ anion and can be explained taking into

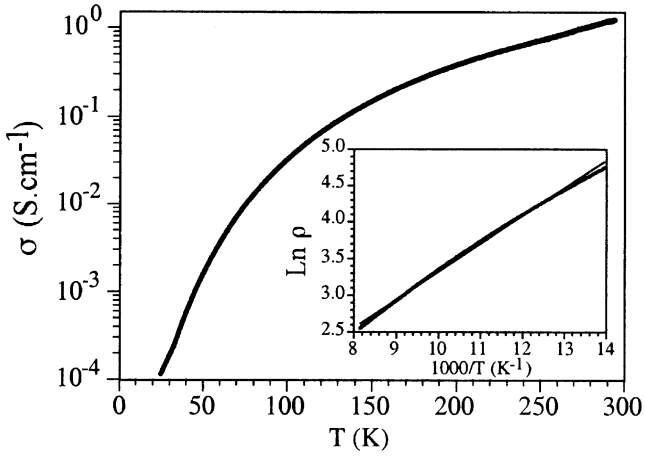

FIG. 5. Logarithmic plot of the thermal variation of the conductivity of the salt $[Ni(dmf)_6][Ni(dsit)_2]_2$. Inset shows the logarithm of the resistivity vs 1000/T.

account the short interdimer Se···Se contacts and the short interchain S···S contacts, which afford a 3-D character to the anion packing (see above). Note that the only examples displaying high conductivities have been found in the compounds $(Z)[Ni(dsit)_2]_2$ ($Z = NMe_4^+$ and PMe_4^+) which contain the mixed-valence $[Ni(dsit)_2]_2^-$ unit and show a two-dimensional (2-D) κ-type acceptor packing (see Table 1).

Electronic Structure

In order to have some insight into the origin of the activated but relatively high conductivity of this salt, we carried out tight-binding band structure calculations for the acceptor sublattice of the salt. As mentioned above, the $Ni(dsit)_2$ molecules are dimerized and there is a 3-D network of relatively short Se···Se and S···S contacts. The repeat unit of the $Ni(dsit)_2$ sublattice contains 12 dimeric units, i.e., the repeat unit of two chains like those shown in Fig. 2. The calculated band structure near the Fermi level is shown in Fig. 6. All of the bands shown in that figure derive from the LUMO of the $Ni(dsit)_2$ although with large contributions of the ligand-based HOMO also. With the formal charge of -1 for $Ni(dsit)_2$, there are 12 electrons to fill the bands of Fig. 6. Consequently, the lower set of six non-dispersive valence bands are filled and there is a band gap at the Fermi level, in agreement with the activated conductivity of this salt. The important result of Fig. 6 is that, in contrast with the non-dispersive nature of the lower bands, the four lower conduction bands exhibit dispersion. Thus the electrons excited to these bands will have a relatively low effective mass, something which presumably is responsible for the high conductivity of the salt. The band gap is somewhat too large in our computations (between two and three times larger since according to the conductivity measurements it should be around 0.07 eV) but in view of the small value of the band gap, a better quantitative agreement is something which is beyond the capabilities of our semiempirical computations. Let us note that the band structure of Fig. 6 is typical for a 1-D semiconductor with better conductivity along the [101] direction, as shown by the dispersive nature of the bands along $\Gamma \rightarrow M$ (i.e., along the $(a^* + c^*)$-direction) but non-dispersive nature along $\Gamma \rightarrow S$ (i.e., along the approximately perpendicular $(-a^* + c^*)$-direction). The semiconducting behavior of this salt is thus governed by the band gap between the filled and upper bands *and* the dispersive nature of the lower empty bands. In order to correlate these facts with the crystal structure of the salt, something which is needed in order to be able to do some crystal engineering with the goal of preparing more conductive $Ni(dsit)_2$-based salts, we need to look more carefully at the nature of the LUMO-based levels of the dimers.

Because of the dimerization, the LUMO of a $Ni(dsit)_2$ unit, which is concentrated in the dsit ligand, interacts with the Ni z^2 orbital of the other $Ni(dsit)_2$ unit of the dimer and is destabilized, leading to a "formally" $\sigma^*_{Ni\cdots Se}$ antibonding level. As shown in Fig. 1, there are two Ni···Se destabilizing interactions per dimer and consequently, there are two such orbitals per dimeric unit. In the following, we will refer to these two orbitals as Ψ_1 and Ψ_2 (although this simplified description is enough for the present discussion, we refer the interested reader to the work by Alvarez et al., (24) for a detailed discussion of the orbital interaction diagram for a $[Ni(dsit)_2]_2^-$ type dimeric unit). From a strictly localized viewpoint, the two $\sigma^*_{Ni\cdots Se}$

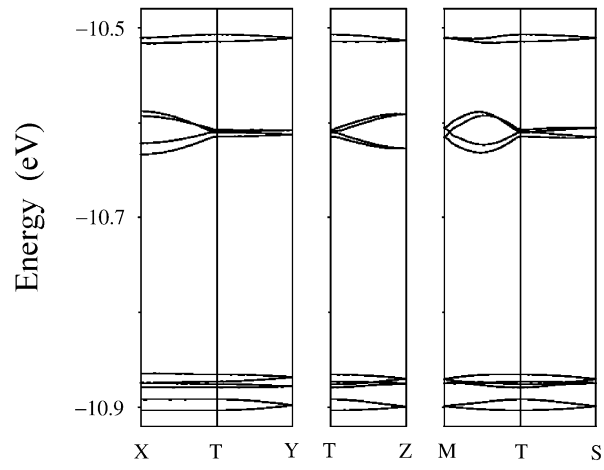

FIG. 6. Calculated band structure near the Fermi level for the $Ni(dsit)_2$ sublattice in $[Ni(dmf)_6][Ni(dsit)_2]_2$, where $\Gamma = (0, 0, 0)$, $X = (a^*/2, 0, 0)$, $Y = (0, b^*/2, 0)$, $Z = (0, 0, c^*/2)$, $M = (a^*/2, 0, c^*/2)$ and $S = (-a^*/2, 0, c^*/2)$.

antibonding levels (i.e., Ψ_1 and Ψ_2) should lie at the same energy. However, because of the proximity of the two bonds and, more importantly, the fact that the two orbitals are really considerably delocalized throughout the ligands, there are always direct as well as indirect interactions through other orbitals of the dsit ligands, so that there is always an energy gap between the two levels. Since Ψ_1 and Ψ_2 lead, respectively, to the upper and lower groups of bands, at least for salts whose structure is not very different from the present one, it seems an inescapable conclusion that, as far as the formal charge of the $[Ni(dsit)_2]_2$ dimeric unit is 2−, the salts built from such dimeric units will be semiconducting. In order to have a metallic behavior, at least one of the two groups of bands should be dispersive enough to override the initial gap due to the energy difference between Ψ_1 and Ψ_2. Under what circumstances could this be possible?

Analysis of the Ψ_1 and Ψ_2 orbitals of the dimers in the present salt shows that, because of the low symmetry of the dimers, in addition to the mixing between orbitals of the different $Ni(dsit)_2$ units, there is a considerable internal orbital mixing among the π-type levels of the same $Ni(dsit)_2$ units (especially with the HOMO which is heavily ligand-based). In other words, there is a considerable polarization of the ligands contribution to Ψ_1 and Ψ_2. The main conclusions of our analysis of the nature of these orbitals are: (a) the upper orbital (Ψ_1) is more heavily concentrated in the two dsit ligands which are implicated in the short Ni···Se intradimer interactions, and (b) the lower orbital (Ψ_2) is more heavily concentrated in the two dsit ligands which are not implicated in the short Ni···Se intradimer interactions. Thus, the Ψ_1 levels will lead to dispersive bands if the Se atoms (and to a lesser extent the S atoms) of the dsit ligands implicated in the short Ni···Se intradimer interactions of one dimer make short contacts with the same type of Se atoms in the neighboring dimers, leading to a continuous path of interdimers short contacts. This is why in the present case the lower empty bands acquire some dispersion and the salt must be a pseudo 1-D semiconductor with better conductivity along the [101] direction. In contrast, the Ψ_2 levels will lead to dispersive bands if the Se atoms (and to a lesser extent the S atoms) of the dsit ligands not implicated in the short Ni···Se intradimer interactions of one dimer make short contacts with the same type of atoms in the neighboring dimers, leading to a continuous path of interdimers short contacts. Of course, making a short contact is a necessary but not sufficient condition: the orientation of the two Se p_z-type orbitals must be appropriate in order to lead to a non-negligible overlap integral. But the existence of short contacts according to the above simple rules is a necessary prerequisite which must be fulfilled in order to have delocalization and thus, band dispersion. Whatever the charge transfer is (i.e., whatever the filling of the Ψ_1 and/or Ψ_2-based bands is), these simple (and approximate) considerations should be useful in the search for more conductive salts based on this kind of dimeric $Ni(dsit)_2$ units.

Magnetic Properties

The magnetic susceptibility shows a Curie behavior with a Curie constant of 1.25 emu $K\,mol^{-1}$. This behavior is typical of isolated Ni(II) ions ($S=1$) with a g value of 2.23 and comes from the contribution of the octahedral $[Ni(dmf)_6]^{2+}$ cations. As expected, the Ni(II) ions in the anionic $[Ni(dsit)_2]_2^{2-}$ dimers do not contribute to the magnetic moment as the delocalized electrons located on each $Ni(dsit)_2$ unit must be strongly antiferromagnetically coupled. Infact they do not present any observable contribution to the magnetic moment, as confirmed also by EPR spectroscopy. An EPR signal coming from the $[Ni(dmf)_6]^{2+}$ octahedral site is also observed at room temperature. This axial signal is quite broad (it ranges from 1000 to 5000 G) and is centered at approximately 2400 G with a second component nearby $g=2$ (Fig. 7). It indicates that the zero-field-splitting of the spin $S=1$ is quite small, in agreement with the high symmetry of the octahedral Ni(II) site in the present case. There is also a very weak signal at $g=2.09$ with a linewidth of 112 G which can be attributed to a very small amount of $[Ni(dsit)_2]^-$ monomers present at the impurity level (12). The isothermal magnetization (Fig. 8) confirms the presence of paramagnetic $S=1$ ions and follows a Brillouin function for a $S=1$ ion with a g value of 2.2.

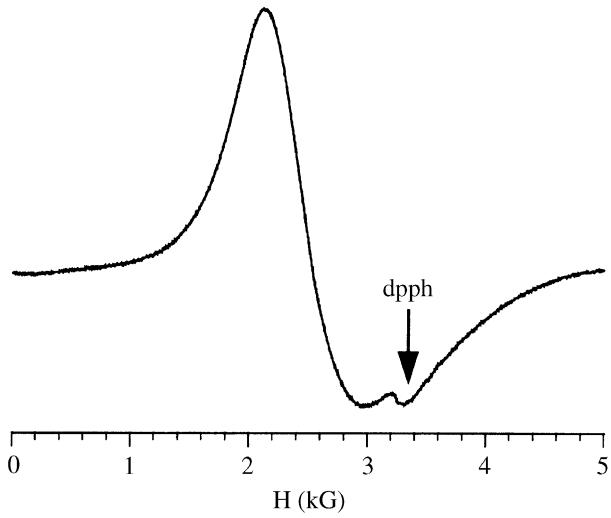

FIG. 7. Room temperature X-band EPR spectrum of the salt $[Ni(dmf)_6][Ni(dsit)_2]_2$).

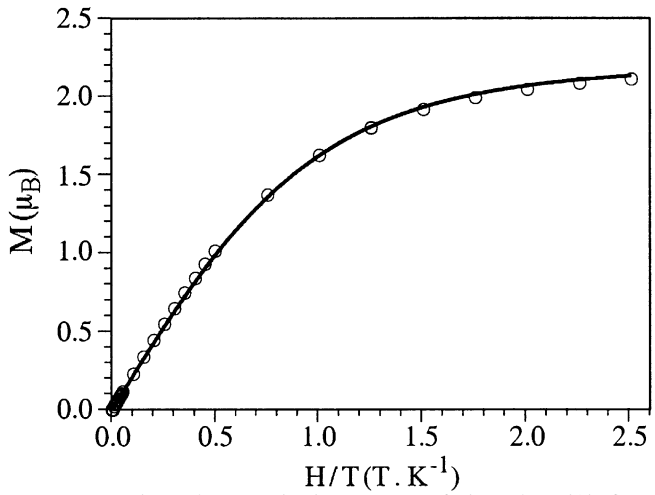

FIG. 8. Isothermal magnetization at 2 K of the salt $[Ni(dmf)_6][Ni(dsit)_2]_2$). Solid line shows the best fit to a Brillouin function for a $S=1$ nickel ion.

CONCLUSIONS

A novel molecular material based on $Ni(dsit)_2$ combining the conducting properties derived from the packing of the anionic $[Ni(dsit)_2]_2^{2-}$ dimers with the paramagnetic properties of Ni(II) cations has been reported. Even if the structural chemistry of $Ni(dsit)_2$ salts is dominated by the formation of dimers, an enhancement in the dimensionality of the solid has been achieved in the present case. Thus, an unprecedented anion packing of $[Ni(dsit)_2]_2^{2-}$ with strong interdimer Se···Se contacts, together with the presence of short S···S interchain contacts have been found. As a consequence, the salt has shown remarkable transport properties with a high room-temperature conductivity, in sharp contrast with the other reported salts based on the $[Ni(dsit)_2]_2^{2-}$ dianion which are insulators. Band structure calculations suggest that the electron carriers should have a relatively low effective mass, and lead to the high conductivity of the salt, due to the existence of Se···Se interdimer contacts between Se atoms of the dsit ligands implicated in the Ni···Se short intradimer interactions.

ACKNOWLEDGMENTS

This work has been developed in the framework of European COST action D14 (project on Inorganic Molecular Conductors). It has been partially supported by CNR, Progetto Materiali Speciali per Tecnologie Avanzate II (Italy), an Italian–Spanish integrated action (HI-0076), DGI-Spain (Project BFM2000-1312-C02-01) and Generalitat de Catalunya (Project 1999 SGR 207).

REFERENCES

1. R. M. Olk, E. Hoyer, C. Faulmann, and P. Cassoux, *Synth. Met.* **56,** 2453 (1993).
2. R. M. Olk, R. Kirmse, E. Hoyer, C. Faulmann, and P. Cassoux, *Z. Anorg. Allg. Chem.* **620,** 90 (1994).
3. M. A. Beno, A. M. Kini, U. Geiser, H. H. Wang, K. D. Carlson, and J. M. Williams, in "The Physics, Chemistry of Organic Superconductors," p. 369. Springer, Berlin, 1990.
4. M. A. Beno, A. M. Kini, S. Budz, H. H. Wang, and J. M. Williams, *Mater. Res. Soc. Symp. Proc.* **173,** 177 (1990).
5. J. P. Cornelissen, J. G. Haasnoot, J. Reedijk, C. Faulmann, J. P. Legros, P. Cassoux, and P. J. Nigrey, *Inorg. Chim. Acta* **202,** 131 (1992).
6. A. Abramov and M. L. Petrov, Zh. *Obshch. Khim.* **66,** 1678 (1996).
7. J. Qin, W. Zhou, Y. Ding, and D. Liu, *Gaodeng Xuexiao Huaxue Xuebao* **13,** 1398 (1992).
8. J. P. Cornelissen, C. Faulmann, J. P. Legros, P. Cassoux, L. Brossard, M. Inokuchi, H. Tajima, and M. Tokumoto, *J. Chem. Soc. Dalton Trans.* 249 (1994).
9. J. P. Cornelissen, J. G. Haasnoot, J. Reedijk, C. Faulmann, J. P. Legros, and P. Cassoux, *Synth. Met.* **56,** 2063 (1993).
10. H. Poleschner, R. Radeglia, and J. Fuchs, *J. Organomet. Chem* **427,** 213 (1992).
11. B. Olk and R. M. Olk, *Z. Anorg. Allg. Chem.* **600,** 89 (1991).
12. R. M. Olk, A. Rohr, J. Sieler, K. Kohler, R. Kirmse, W. Dietzsch, E. Hoyer, and B. Olk, *Z. Anorg. Allg. Chem.* **577,** 206 (1989).
13. P. J. Nigrey, *Synth. Met.* **27,** B365 (1988).
14. N. Walker and D. Stuart, *Acta Crystallogr. A* **39,** 158 (1983).
15. A. Altomare, C. Cascarano, C. Giacovazzo, A. Guagliardi, M. C. Burla, G. Polidori, and M. Camalli, *J. Appl. Crystallogr.* **27,** 435 (1994).
16. G. M. Sheldrick, "SHELXL-97: Program for Crystal Structure Refinement," University of Göttingen, Göttingen, Germany, 1997.
17. (a) M. H. Whangbo and R. Hoffmann, *J. Am. Chem. Soc.* **100,** 6093 (1978); (b) R. Hoffmann, *J. Chem. Phys.* **39,** 1397 (1963).
18. J. Ammeter, H. B. Bürgi, J. Thibeault, and R. Hoffmann, *J. Am. Chem. Soc.* **100,** 3686 (1978).
19. E. Canadell, I. E. I. Rachidi, S. Ravy, J. P. Pouget, L. Brossard, and J. P. Legros, *J. Phys. France* **50,** 2967 (1989).
20. E. Canadell, A. LeBeuze, M. A. El Khalifa, R. Chevrel, and M. H. Whangbo, *J. Am. Chem. Soc.* **111,** 3778 (1989).
21. V. Mc Kee, T. Metcalfe, and J. Wikaira, *Acta Crystallogr. C* **52,** 1139 (1996).
22. W. S. Li, A. J. Blake, N. R. Champness, M. Schröder, and D. W. Bruce, *Acta Crystallogr. C* **54,** 349 (1998).
23. K. I. Pokhodnya, C. Faulmann, I. Malfant, R. Andreu-Solano, P. Cassoux, A. Mlayah, D. Smirnov, and J. Leotin, *Synth. Met.* **55,** 1253 (1999).
24. S. Alvarez, R. Vicente, and R. Hoffmann, *J. Am. Chem. Soc.* **107,** 6253 (1985).